Supporting Information

Direct construction interconnected Si_3N_4 nanowires networks for enhancing thermal conductivity and mechanical performance of flexible composite films

Mengyi Li[a], Baokai Wang[a], Chang Yu[a], Mengyang Niu[a], Kunjie Yuan[a], Weiwei Xuan[b], Ming Yue[c], Lifeng Zhu[a,*] Kexin Chen[d,*], Qi Wang[a,*]

[a] *School of Materials Science and Engineering, University of Science and Technology Beijing, Beijing 100083, China*

[b] *School of Energy and Environmental Engineering, University of Science and Technology Beijing, Beijing 100083, China*

[c] *School of Civil and Resource Engineering, University of Science and Technology Beijing, Beijing 100083, China*

[d] *State Key Laboratory for Advanced Metals and Materials, University of Science and Technology Beijing, Beijing, 100083, China*

*Corresponding authors: zhu@ustb.edu.cn (L. Zhu), kxchen@ustb.edu.cn (K. Chen), wangqi15@ustb.edu.cn (Q. Wang)

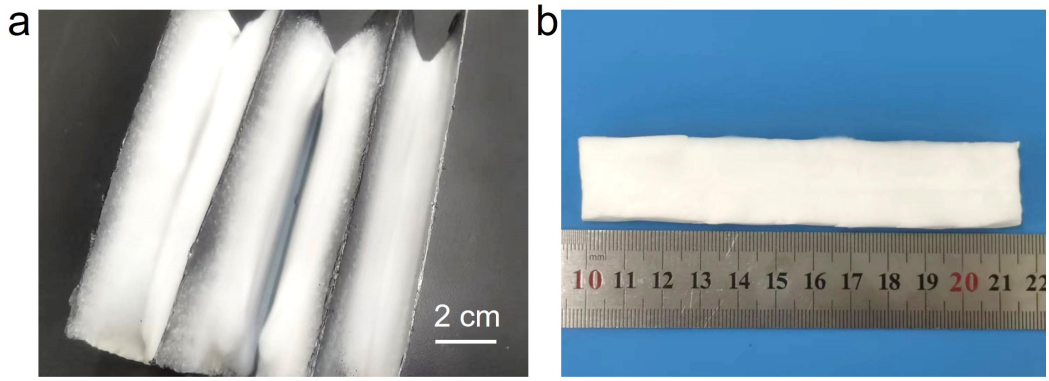

Fig. S1 (a) Digital pictures showing the Si_3N_4NWs grown on the substrate of carbon paper; (b) digital picture of a large piece of Si_3N_4NWs paper after detaching.

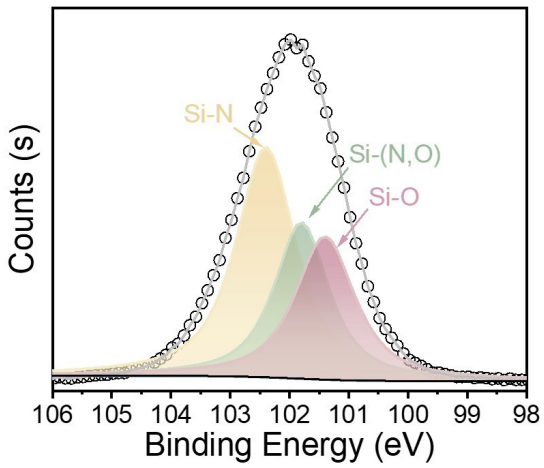

Fig. S2 High-resolution XPS spectrum of Si 2p.

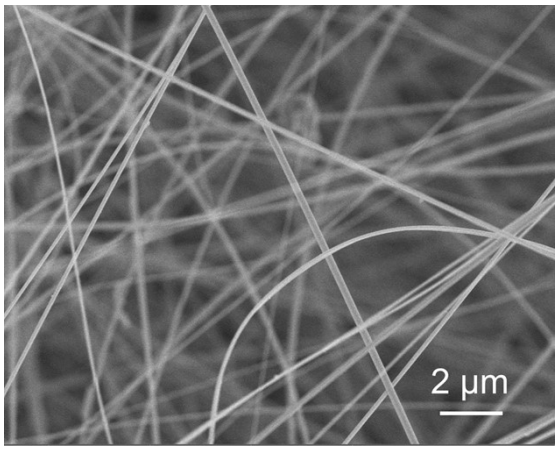

Fig. S3 SEM image of the as-synthesized Si_3N_4NWs paper.

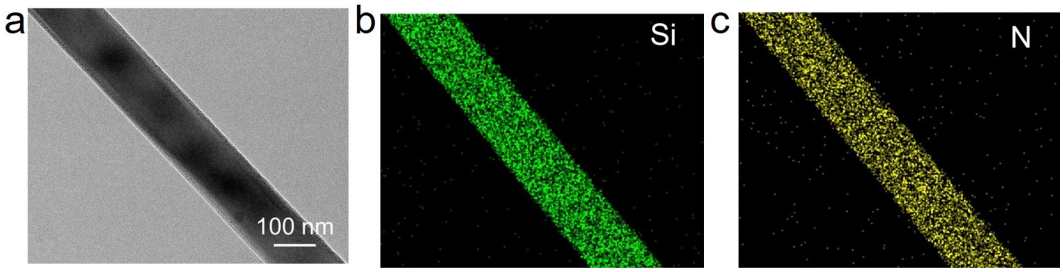

Fig. S4 (a) TEM image of single Si_3N_4NW; corresponding EDS mapping images of (b) Si and (c) N elements.

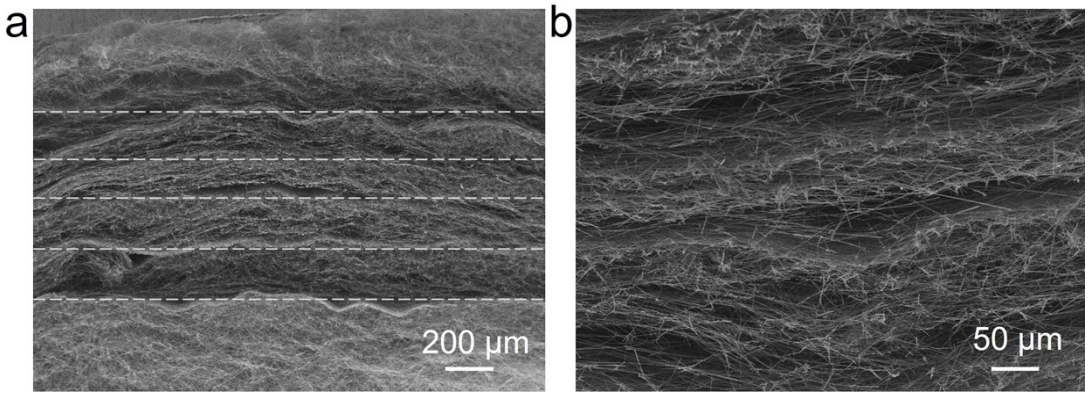

Fig. S5 Cross-sectional SEM image of the six-layer stacked Si_3N_4NWs paper under different magnifications: (a) 100×, (b) 500×.

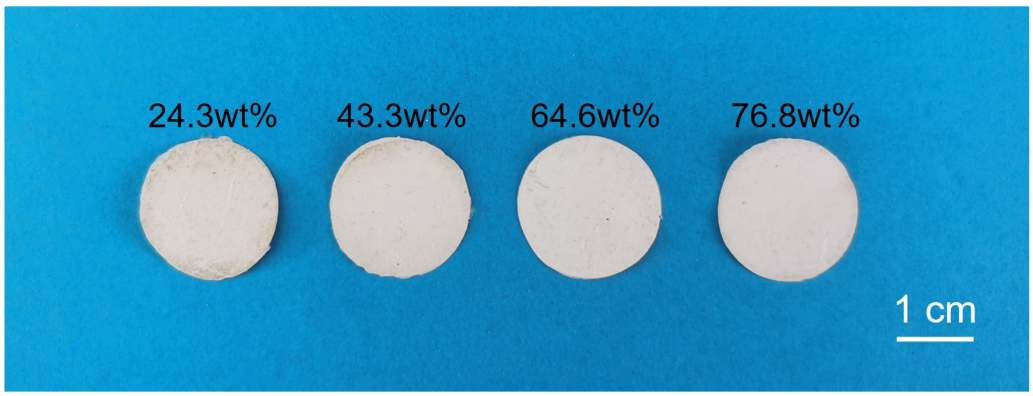

Fig. S6 Digital pictures of various Si_3N_4NWs/EP composite films with different filling fractions.

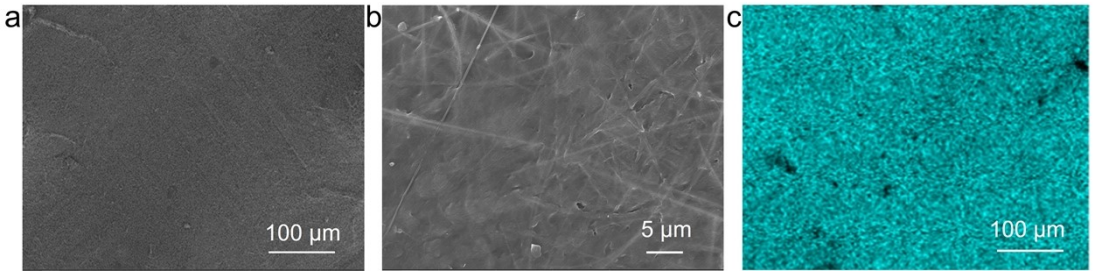

Fig. S7 (a-b) SEM images at different magnifications and (c) Si elemental distribution on the surface of the 64.6L-Si_3N_4NWs/EP composite film.

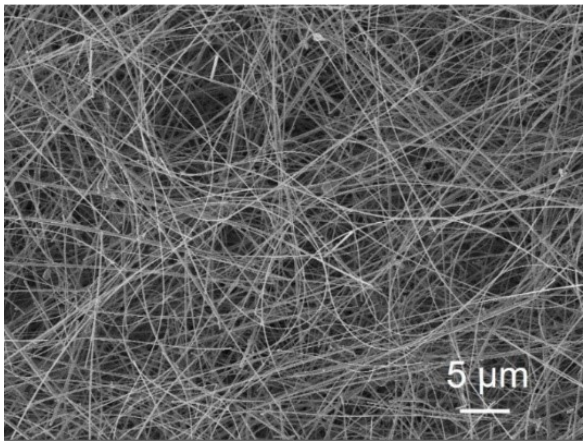

Fig. S8 SEM image of the residual Si_3N_4NWs skeleton of the composite film after heat treatment at 800 °C for 2 h in air atmosphere.

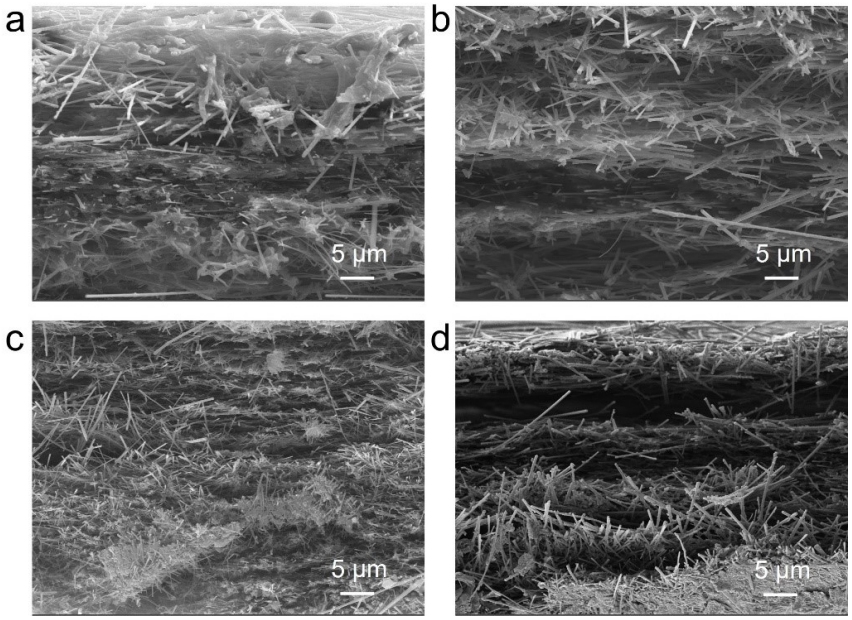

Fig. S9 SEM images of fracture surfaces of composite films with different Si_3N_4NWs filling fraction: (a) 24.3 wt%; (b) 43.3 wt%; (c) 64.6 wt%; (d) 76.8 wt%.

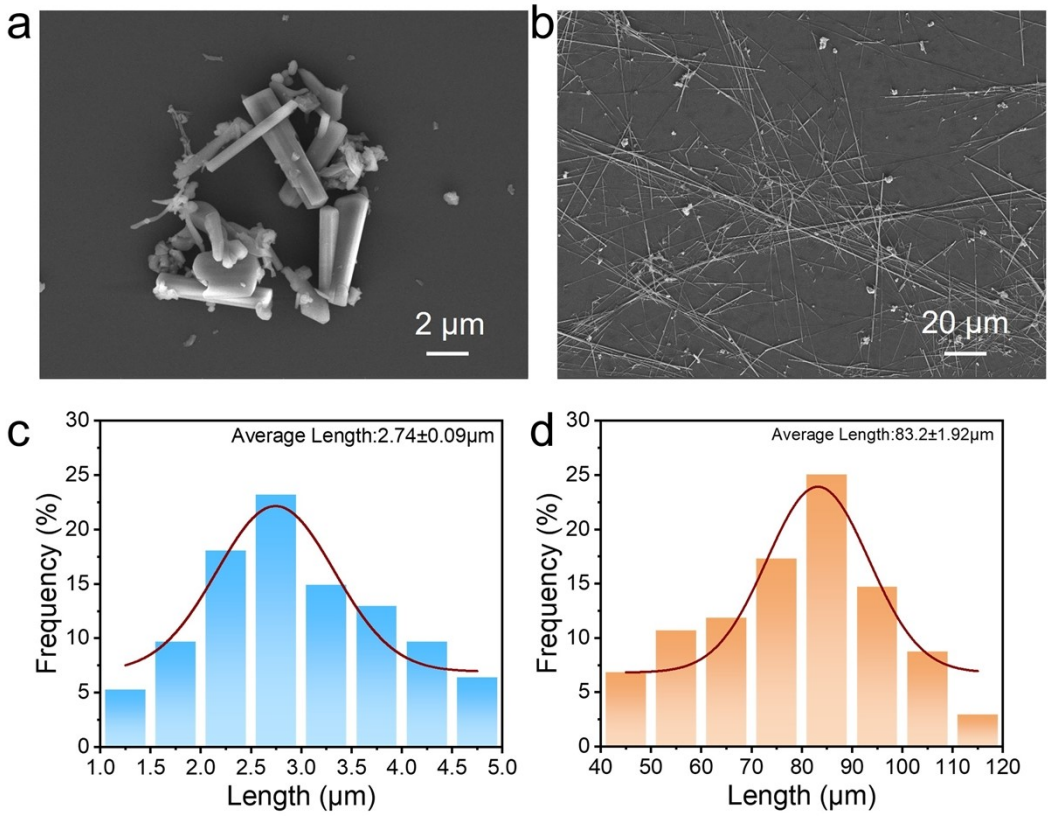

Fig. S10 SEM images and length distribution of Si_3N_4Ps and S-Si_3N_4NWs: (a,c) Si_3N_4Ps; (b,d) S-Si_3N_4NWs.

Tab. S1 Density and porosity of *x*L-Si_3N_4NWs/EP composite films

Composite films samples	Calculated density (g/cm^3)	Measured density (g/cm^3)	Porosity (vol%)
24.3L-Si_3N_4NWs/EP	1.4255	1.3778	3.14
43.3L-Si_3N_4NWs/EP	1.7052	1.5521	8.97
64.6L-Si_3N_4NWs/EP	1.9244	1.7341	9.89
76.8L-Si_3N_4NWs/EP	2.3455	1.4246	39.11

Tab. S2 Comparison of the comprehensive performance between the as-prepared 64.6L-Si_3N_4NWs/EP composite film and some previously reported composite films.

Composites	In-plane TC ($W \cdot m^{-1} \cdot K^{-1}$)	Through-plane TC ($W \cdot m^{-1} \cdot K^{-1}$)	Tensile stress (Mpa)	Tensile strain (%)	Volume resistivity ($\Omega \cdot cm$)	References
AlN/ UHMWPE	7.12	1.93	16.8	/	/	2023[S1]
PVDF/BN/PW	0.52	/	/	/	1.89×10^5	2024[S2]
NH_2-rGO/ PI	7.13	0.74	35.7	/	/	2021[S3]
Si_3N_4NWs/PVA	15.4	1.52	3.4	/	/	2023[S4]
Si_3N_4NWs/EP	16.02	2.21	37.3	10.17	6.68×10^9	This work

[S1] S. Wan, X. Hao, C. Yu, M. Li, Z. Zhao, L, Zhu, W. Xuan, M. Yue, W. Cao and Q. Wang, Ceram. Int., 2023, 49, 35094-35103.

[S2] K. Ruan, Y. Guo, C. Lu, X. Shi, T. Ma, Y. Zhang, J. Kong and J. Gu, Research, 2021, 2021: 8438614.

[S3] X. Zhang, K. Sun, H. Liu, J. Chen, X. Yan, Y. Kou and Q. Shi, Nano Energy, 2024, 121, 109256.

[S4] S. Wan, X. Hao, L. Zhu, C. Yu, M. Li, Z. Zhao, J. Kuang, M. Yue, Q. Lu, W. Cao, and Q. Wang, ACS Appl. Mater. Interfaces, 2023, 15, 32885-32894.